JACS
JOURNAL OF THE AMERICAN CHEMICAL SOCIETY

COMMUNICATION

pubs.acs.org/JACS

Leading Neuroblastoma Cells To Die by Multiple Premeditated Attacks from a Multifunctionalized Nanoconstruct

Peifu Jiao,[†,∥] Hongyu Zhou,[∥] Mario Otto,[§] Qingxin Mu,[∥] Liwen Li,[‡,∥] Gaoxing Su,[‡,∥] Yi Zhang,[†,∥] Elizabeth R. Butch,[#] Scott E. Snyder,[#] Guibin Jiang,[⊥] and Bing Yan[*,‡,∥]

[†]School of Pharmaceutical Sciences and [‡]School of Chemistry and Chemical Engineering, Shandong University, Jinan, Shandong 250012, China

Departments of [∥]Chemical Biology and Therapeutics, [§]Oncology, and [#]Radiological Sciences, St. Jude Children's Research Hospital, Memphis, Tennessee 38105, United States

[⊥]Research Center for Eco-Environmental Sciences, Chinese Academy of Sciences, Beijing 100085, China

Supporting Information

ABSTRACT: To conquer complex and devastating diseases such as cancer, more coordinated and combined attack strategies are needed. We suggest that these can be beautifully achieved by using nanoconstruct design. We present an example showing that neuroblastoma cells are selectively killed by a nanoconstruct that specifically targets neuroblastoma cells, pushes cells to the vulnerable phase of the cell cycle, and greatly enhances radiation-induced cell death. The success of this multipronged attack approach launched by cell-embedded nanoconstructs demonstrates the power and flexibility of nanotechnology in treating cancer, a difficult task for a small molecule.

Cancer is a deadly disease with high complexity. Multipronged and coordinated approaches are needed to conquer this devastating disease. Because of intrinsic limitations, it is difficult to build multiple capabilities into a single small molecule; however, it is possible to equip a nanoconstruct with multiple arsenals. Among these arsenals, chemical and biological agents can be launched one-by-one to stage multiple attacks on cancer cells in a coordinated effort to kill cells. Here we report a cancer-targeting, cell-modulating, radiation-enhancing, biocompatible nanoconstruct that strategically kills neuroblastoma cells with high specificity.

Neuroblastoma is the most common extracranial solid tumor in childhood.[1] More than 50% of neuroblastoma cases occur in children younger than 2 years old. As a disease of the sympaticoadrenal lineage of the neural crest, tumors can develop anywhere in the sympathetic nervous system.[2] Current treatments, including surgery, chemotherapy, radiation, and stem cell transplantation, induce significant side effects such as growth delays, hearing loss, and learning disabilities. Despite multimodality therapy, many patients with advanced-stage disease ultimately succumb to relapse. Therefore, more effective and cancer-specific therapy is urgently needed, especially for this fragile patient population.

GD2 disialoganglioside is an antigen expressed on tumors of neuroectodermal origin, including neuroblastoma,[3−5] with a highly restricted expression on normal tissues.[6] Hu14.18K322A is a humanized anti-GD2 antibody currently being investigated in a phase-I immunotherapy study in neuroblastoma patients at St. Jude Children's Research Hospital.[7] This antibody binds to GD2 specifically and causes antibody-dependent cytotoxicity but much less complement activation than the related chimeric anti-GD2 antibody, ch14.18,[8,9] which is currently the focus of an immunotherapy trial by the Children's Oncology Group.[10] We incorporated hu14.18K322A into our nanoconstruct as a targeting moiety to recognize neuroblastoma cells while avoiding normal cells.

We and others have previously shown that gold nanoparticles (GNPs), like other elements with high atomic number (Z), enhance radiation-induced cell death.[11−17] All cells are not equally sensitive to radiation during all stages of the cell cycle.[18] For example, cells are radiation-resistant in the S phase, whereas they become very sensitive to radiation in the G2/M phase.[19,20] An agent that arrests cells at the G2/M phase of the cell cycle, such as paclitaxel (PTX), would thus be an effective chemical weapon to make cells vulnerable to radiation. To carry out a specific lethal assault on cancer cells while sparing normal cells, we designed a nanoconstruct-initiated three-strike approach. First, neuroblastoma cells are specifically targeted. Next, cells are artificially arrested in the G2/M phase of the cell cycle. Finally, the cancer cells are killed by the enhanced radiation cytotoxicity.

To assemble a nanoconstruct with these multiple arsenals, we first prepared thiol-linker-containing hu14.18K322A antibody along with β-cyclodextrin (β-CD) for paclitaxel loading. Through Au−S bonding, they were all incorporated into GNPs along with PEG polymers to form hu14.18K322A-targeted GNPs (HGNPs) and hu14.18K322A-targeted, PTX-loaded GNPs (HPGNPs) [see the Supporting Information (SI) for details].

The number of hu14.18K322A molecules on each GNP was determined by elemental analysis of nitrogen content (%) in a given amount of nanoconstructs. To determine the number of PTX molecules on each HPGNP, LC−MS analysis was used to quantify the amount of PTX remaining after the drug was loaded onto the HPGNPs. There were 16 hu14.18K322A molecules and ∼11 PTX molecules on each HPGNP (Table 1 and Figure S3 in the SI). The diameter of a bare GNP was ∼15 nm on the basis of transmission electron microscopy (TEM) measurements (Table 1, Figure 1a, and Figure S2). Phosphotungstic acid (PTA) was used to stain hu14.18K322A on the surface of the GNPs, enabling the visualization of GNP-bound hu14.18K322A

Received: July 1, 2011
Published: August 09, 2011

Table 1. Characteristics of GNPs, Hu14.18K322A, HGNPs, and HPGNPs

sample	avg size (nm)[a]	number per GNP: hu14.18K322A[b]	number per GNP: PTX[c]
GNPs	15 ± 5	–	–
hu14.18K322A	12 ± 3	–	–
HGNPs	50 ± 10	16	–
HPGNPs	50 ± 15	16	11

[a] Determined by DLS analysis (Figure S2). [b] Determined by elemental analysis (Figure S3). [c] Determined by HPLC−MS (Figure S3).

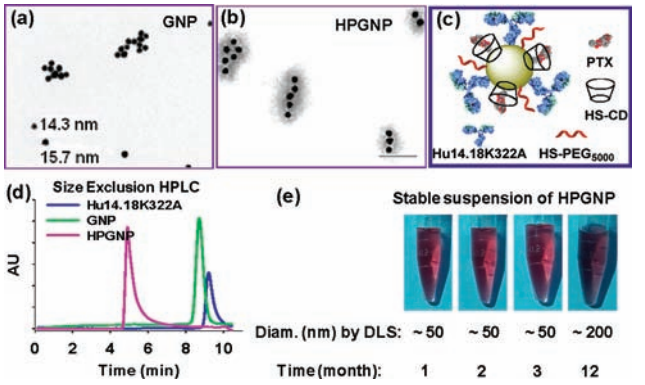

Figure 1. Characterization of HPGNPs. (a, b) TEM images of (a) bare GNPs and (b) HPGNPs (stained with 2% PTA, pH 6.0, scale bar 100 nm). (c) Structure of an HPGNP. (d) SEC−HPLC traces (mobile phase: 3 mM sodium citrate). (e) Stability of HPGNPs in phosphate-buffered saline at 4 °C.

molecules (Figure 1b). The dark clouds around the GNPs represent molecular backbones of hu14.18K322A. The little white dots closer to the GNP surface are molecules that could not be stained by PTA, such as bound CD, loaded PTX, PEG units, and polysaccharides in the Fc domain of hu14.18K322A. Furthermore, the distances between adjacent HPGNPs were larger than those between adjacent GNPs, suggesting that hu14.18K322A molecules were conjugated to the GNPs. Dynamic light scattering (DLS) was used to measure the hydrodynamic size of the particles in an aqueous solution (Figure S2). The diameter of a bare GNP was 15 ± 5 nm, in agreement with the sizes obtained using TEM. After conjugation with hu14.18K322A (12 ± 3 nm in diameter), PEG thiol (HS-PEG, MW 5000 Da), and thiol-appended β-CD (HS-β-CD), the hydrodynamic diameter of the GNPs increased to 50 ± 15 nm. Size-exclusion chromatography−HPLC (SEC−HPLC) analysis also showed the size increase (evidenced by early elution; Figure 1d). Because free hu14.18K322A molecules in the HPGNP solution might hinder the targeting efficiency of HPGNP in GD2-positive tumor cells, excess antibodies were completely removed by six rounds of washing and centrifugation. The presence of pure HPGNPs without any free antibody was confirmed by the SEC−HPLC results (Figure 1d).

Cells may express various levels of GD2 antigens on their surface. Using a fluorescent secondary antibody and flow cytometry, we measured the amount of GD2 expression on the surface of CHLA-20, IMR32, and PC-3 cells. We found that the neuroblastoma cell lines, CHLA-20 and IMR32, were both GD2-positive, although the expression of GD2 in IMR32 [mean fluorescence intensity (MFI) = 7304] was only 77% of that in CHLA-20 (MFI = 9554; Figure S4). PC-3, a human prostate cancer cell line, did not have any detectable GD2 (MFI = 120), as previously reported.[21,22] It is therefore a good representative of normal cells and was used as negative control.

With nanoconstructs made and cell lines selected, our first test was to determine whether HPGNPs specifically target neuroblastoma cells by avoiding cells that do not express the GD2 antigen, such as normal cells. Dark-field microscopy images showed that HPGNPs accumulated abundantly in GD2-positive cells but not in GD2-negative cells (Figure S7). Additional ultrastructural details of the time-dependent cellular uptake of HPGNPs were provided by TEM. After a 4 h incubation of cells with HPGNP, individual particles were selectively bound to IMR32 and CHLA-20 plasma membranes (Figure 2b,c) but not to a PC-3 membrane, indicating specific GD2 recognition and binding. At 12 h, bound HPGNPs were internalized by cells. The internalized HPGNPs were localized in endosomal- or lysosomal-like organelles and also in the cytoplasm, indicating that they might enter cells by penetrating the plasma membrane or by breaking endosomal membranes. Membranes of some endosomes or lysosomes were actually ruptured (arrows in Figure 2e,f). This is very interesting, although we currently have no explanation for this observation. Furthermore, we also found particles in the cytoplasm at 4 h, when endosomal membranes were not ruptured (Figure 2c inset).

We next analyzed cellular gold content by using ICP-MS to evaluate quantitatively the cells' recognition and internalization of HPGNPs. CHLA-20 and IMR32 cells had 60- and 50-fold more HPGNPs, respectively, than did GD2-negative PC-3 cells (Figure 2g,h), indicating extremely high selectivity. Additionally, the average uptake rate of CHLA-20 cells ($k_{\text{CHLA-20}}$ = 1.4820) was 1.4-fold higher than that of IMR32 cells (k_{IMR32} = 1.0881) (Figure S5), suggesting that the amount of GD2 expression on the cell surface played a role in accelerating the cell uptake of HPGNPs. The amounts of internalized HPGNPs reached plateaus at 24 h when the HPGNP concentration was 2.5 nM, indicating that the cellular concentrations of HPGNPs finally reached a steady state (Figure 2h). At equilibrium, the total internalized HPGNP contents of CHLA-20 and IMR32 cells were 62- and 48-fold higher, respectively, than those of PEG−GNPs in the corresponding cells (nonspecific uptake; Figure S6). This result suggested that the hu14.18K322A−GD2 interaction was responsible for the specific uptake of HPGNPs by GD2-positive cells. To provide further confirmation that the recognition of HPGNPs by GD2-positive neuroblastoma cells was a result of GD2−hu14.18K322A interactions, an antibody competition experiment was performed. CHLA-20 cells were pretreated with free hu14.18K322A for 4 h and then treated with HPGNPs. The cellular uptake of HPGNPs was quantitatively evaluated using ICP-MS (Figure 2i). The HPGNP uptake by CHLA-20 was nearly blocked by 25−100 nM free hu14.18K322A. Such a blockade was also confirmed by TEM analysis (Figure 2j,k). In the presence of 25 nM hu14.18K322A, fewer HPGNPs were bound to cells or internalized. These results demonstrate that the enhanced cell recognition in GD2-positive neuroblastoma cells was a direct result of GD2−hu14.18K322A interactions.

After HPGNPs were specifically internalized into neuroblastoma cells through hu14.18K322A−GD2 interactions, they were ready to push cells into the G2/M phase by delivering PTX molecules to intracellular targets (i.e., tubulins). As shown in Figure 3, the HPGNPs arrested 68% of the CHLA-20 cells in the G2/M phase at 12 h, whereas PTX caused only a 44% G2/M arrest rate. Similar results were seen for IMR32 cells. In PC-3 cells, free PTX caused

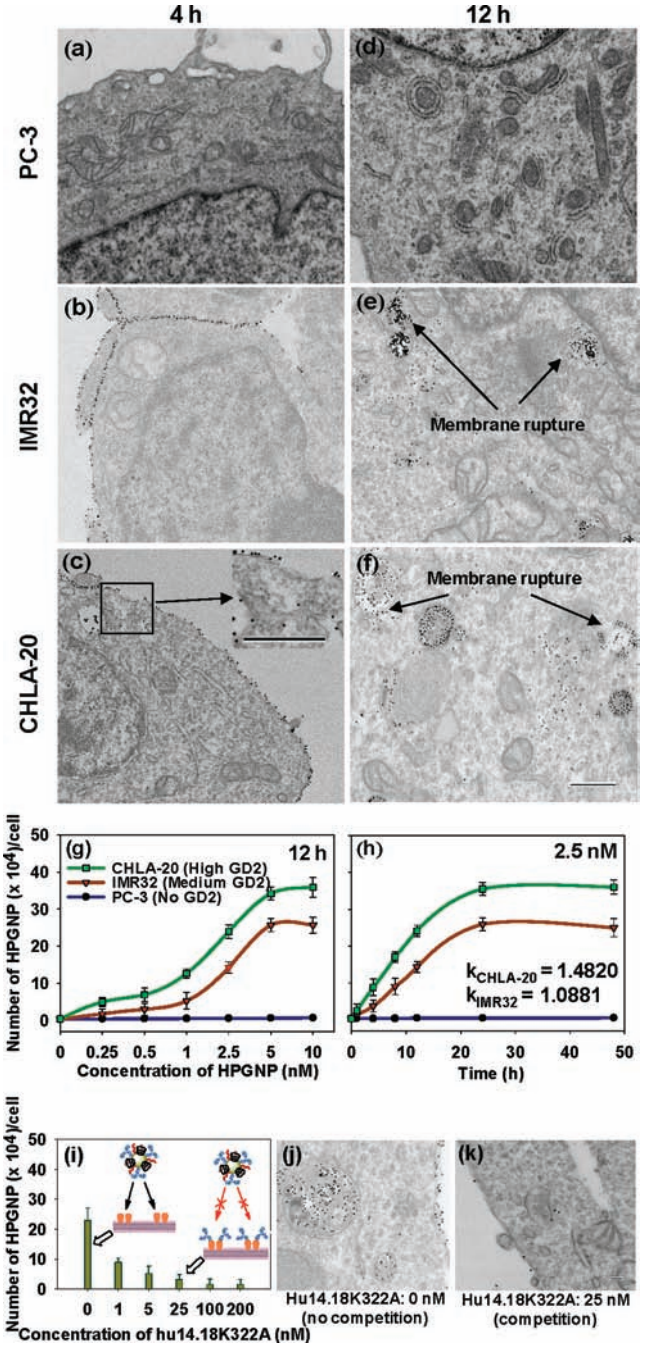

Figure 2. HPGNP recognition by and internalization into neuroblastoma cells. (a−f) TEM images revealing the targeting process and cellular distribution of HPGNPs (2.5 nM) in neuroblastoma cells and GD2-negative PC-3 cells (scale bar 500 nm). (g) Dose-dependent cellular uptake of HPGNPs in neuroblastoma cells and GD2-negative PC-3 cells (incubation time 12 h). (h) Time-dependent cellular uptake of HPGNPs in neuroblastoma cells and GD2-negative PC-3 cells (2.5 nM). (i) Cellular uptake of HPGNPs (2.5 nM) in CHLA-20 cells pretreated with hu14.18K322A for 4 h and then with HPGNPs for 12 h. (j, k) TEM images of CHLA-20 cells pretreated with free antibody (0 and 25 nM) for 4 h and then treated with HPGNPs (2.5 nM) for 12 h (scale bar 100 nm).

significant cell-cycle arrest at the G2/M phase (43%). However, HPGNPs did not induce G2/M arrest, suggesting that HPGNPs effectively blocked the cellular uptake of PTX by GD2-negative cells. A major and critical mechanism of drug resistance in cancer cells is

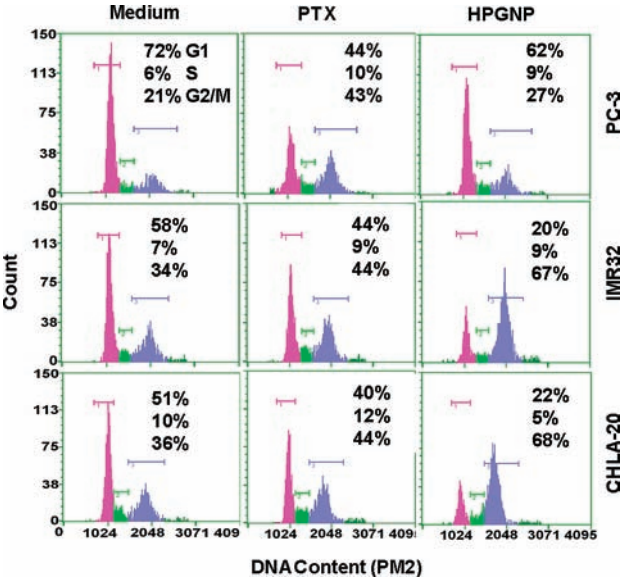

Figure 3. Induction of G2/M arrest by HPGNPs (PTX content 11 nM, 12 h) and PTX (11 nM, 12 h) in GD2-negative cells and neuroblastoma cells.

the up-regulation of ABC transporter genes, which leads to the rapid elimination of various cytotoxic agents, including taxols.[23] IMR32 and CHLA-20 cells are multi-drug-resistant cell lines that utilize this mechanism.[24,25] As an alternative explanation for the increased G2/M arrest rate conferred by HPGNPs, one could thus speculate that intracellular HGNP-bound PTX may at least partially evade rapid elimination mediated by ABC transporters and increase its cytotoxic effects, as we observed in our experiments. In sum, these results demonstrate that the GD2-targeting HPGNPs can specifically deliver PTX to neuroblastoma cells to induce cell-cycle arrest without affecting GD2-negative cells (i.e., normal cells).

Once HPGNPs specifically brought cells to the vulnerable G2/M phase, we aimed to kill neuroblastoma cells using radiation, taking advantage of the enhanced radiation effects caused by HPGNPs and the enhanced vulnerability of dividing cells. HGNPs alone showed no cytotoxicity to either GD2-positive or -negative cells, indicating a high degree of biocompatibility (Figure 4a−c). As expected, HGNPs enhanced the radiation-induced cell death in GD2-positive neuroblastoma cells (Figure 4b,c and Figure S10). Both CHLA-20 and IMR32 cells have been reported to be drug-resistant,[26−28] especially to PTX. According to our results, PTX (11 nM) did not cause much toxicity to these cell lines after 12 h (Figure 4e,f). However, incubation of cells with HPGNPs without radiation induced more cell death under the same conditions (Figure 4h,i and Figure S9), suggesting that cancer-targeting HPGNPs transported many more PTX molecules into neuroblastoma cells and possibly evaded efflux generated by ABC transporters. HPGNPs were not toxic to PC-3 cells (Figure 4g), although the PTX was highly toxic under the same conditions (Figure 4d). This result strongly demonstrates that the HPGNPs effectively reduced the toxicity of PTX to GD2-negative cells by evading them. Because HPGNP caused neuroblastoma cells to pause at the G2/M phase, radiation treatment became much more effective, thus doubling the cell death (Figure 4h,i and Figure S9).

In summary, we have designed and assembled a novel nanoconstruct, HPGNPs, with multipronged attack capabilities specifically targeted to neuroblastoma cells. HPGNPs accomplish three key strikes: they specifically target neuroblastoma cells;

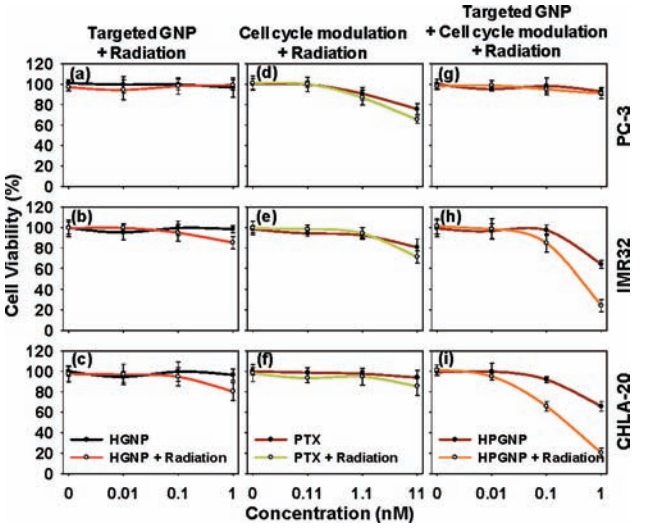

Figure 4. Enhancement of radiation cytotoxicity to neuroblastoma cells by HPGNPs. All cells were treated with or without HGNP, PTX, and HPGNP for 12 h. After exposure to X-rays (3 Gy dose), all particles or drugs were removed, and fresh medium was added. After another 48 h, cell viability was measured using the WST-1 method. The concentrations of HPGNPs in (g–i) were kept the same as that of HGNPs, so the PTX concentrations on HPGNPs were identical to those in (d–f).

drive them to the G2/M phase of the cell cycle, thus making them highly vulnerable to radiation; and significantly enhance radiation-induced cell death. HPGNPs did not bind GD2-negative cells and caused little toxicity or radiation-induced cell death in these cells. Our data demonstrate the power and flexibility of nanotechnology in treating complex diseases such as cancer by using multiple strategies to attack cancer cells from multifunctional nanoconstructs, a task that is difficult to achieve by using a small molecule alone.

■ ASSOCIATED CONTENT

Supporting Information. Preparation and characterization of GNPs, HGNPs, HPGNPs, and β-CD derivatives; cell culture; GD2 expression measurement; cellular uptake of HPGNPs; competition experiment with free hu14.18K322A; dark-field microscopy; TEM; release of PTX; cell cycle assay; cytotoxicity assay; and complete ref 10. This material is available free of charge via the Internet at http://pubs.acs.org.

■ AUTHOR INFORMATION

Corresponding Author
dr.bingyan@gmail.com

■ ACKNOWLEDGMENT

We thank Sharon Frase, Linda Mann, Jennifer Peters, Tom Mohaupt, and Richard Ashmun for technical assistance and Merck KGaA for the generous gift of hu14.18K322A antibody. We also thank Cherise M. Guess for editing and checking the text of the manuscript. This work was supported by the National Basic Research Program of China (2010CB933504), the National Natural Science Foundation of China (90913006 and 21077068), the National Cancer Institute (P30CA027165), and the American Lebanese Syrian Associated Charities (ALSAC).

■ REFERENCES

(1) Baker, D. L.; Schmidt, M. L.; Cohn, S. L.; Maris, J. M.; London, W. B.; Buxton, A.; Stram, D.; Castleberry, R. P.; Shimada, H.; Sandler, A.; Shamberger, R. C.; Look, A. T.; Reynolds, C. P.; Seeger, R. C.; Matthay, K. K. *New Engl. J. Med.* **2010**, *363*, 1313.
(2) Maris, J. M.; Hogarty, M. D.; Bagatell, R.; Cohn, S. L. *Lancet* **2007**, *369*, 2106.
(3) Mujoo, K.; Cheresh, D. A.; Yang, H. M.; Reisfeld, R. A. *Cancer Res.* **1987**, *47*, 1098.
(4) Cheung, N. K. V.; Saarinen, U. M.; Neely, J. E.; Landmeier, B.; Donovan, D.; Coccia, P. F. *Cancer Res.* **1985**, *45*, 2642.
(5) Kramer, K.; Gerald, W. L.; Kushner, B. H.; Larson, S. M.; Hameed, M.; Cheung, N. K. V. *Med. Pediatr. Oncol.* **2001**, *36*, 194.
(6) Svennerholm, L.; Bostrom, K.; Fredman, P.; Jungbjer, B.; Lekman, A.; Mansson, J. E.; Rynmark, B. M. *Biochem. Biophys. Acta* **1994**, *1214*, 115.
(7) Navid, F.; Barfield, R. C.; Handgretinger, R.; Sondel, P. M.; Shulkin, B. L.; Kaufman, R.; Billups, C.; Wu, J.; Furman, W. L.; McGregor, L. M.; Otto, M.; Gillies, S.; Santana, V. M. *J. Clin. Oncol.* **2011**, *29* (Suppl.), 9523.
(8) Navid, F.; Santana, V. M.; Barfield, R. C. *Curr. Cancer Drug Targets* **2010**, *10*, 200.
(9) Sorkin, L. S.; Otto, M.; Baldwin, W. M.; Vail, E.; Gillies, S. D.; Handgretinger, R.; Barfield, R. C.; Yu, H. M.; Yu, A. L. *Pain* **2010**, *149*, 135.
(10) Yu, A. L.; et al. *New Engl. J. Med.* **2010**, *363*, 1324.
(11) Li, X.; Zhou, H.; Yang, L.; Du, G.; Pai-Panandiker, A. S.; Huang, X.; Yan, B. *Biomaterials* **2011**, *32*, 2540 .
(12) Zhou, H. Y.; Jiao, P. F.; Yang, L.; Li, X.; Yan, B. *J. Am. Chem. Soc.* **2011**, *133*, 680.
(13) Chattopadhyay, N.; Cai, Z. L.; Pignol, J. P.; Keller, B.; Lechtman, E.; Bendayan, R.; Reilly, R. M. *Mol. Pharmaceutics* **2010**, *7*, 2194.
(14) Hainfeld, J. F.; Dilmanian, F. A.; Zhong, Z.; Slatkin, D. N.; Kalef-Ezra, J. A.; Smilowitz, H. M. *Phys. Med. Biol.* **2010**, *55*, 3045.
(15) Jiao, P. F.; Zhou, H. Y.; Chen, L. X.; Yan, B. *Curr. Med. Chem.* **2011**, *18*, 2086.
(16) Jelveh, S.; Chithrani, D. B. *Cancers* **2011**, *3*, 1081.
(17) Chithrani, D. B.; Jelveh, S.; Jalali, F.; van Prooijen, M.; Allen, C.; Bristow, R. G.; Hill, R. P.; Jaffray, D. A. *Radiat. Res.* **2010**, *173*, 719.
(18) Terasima, T.; Tolmach, L. J. *Nature* **1961**, *190*, 1210.
(19) Dunne, A. L.; Mothersill, C.; Robson, T.; Wilson, G. D.; Hirst, D. G. *Oncol. Res.* **2004**, *14*, 447.
(20) Hennequin, C. *Cancer Radiother.* **2004**, *8* (Suppl. 1), S95.
(21) Voss, S. D.; Smith, S. V.; DiBartolo, N.; McIntosh, L. J.; Cyr, E. M.; Bonab, A. A.; Dearling, J. L.; Carter, E. A.; Fischman, A. J.; Treves, S. T.; Gillies, S. D.; Sargeson, A. M.; Huston, J. S.; Packard, A. B. *Proc. Natl. Acad. Sci. U.S.A.* **2007**, *104*, 17489.
(22) Vavere, A.; Butch, E.; Dearling, J.; Packard, A.; Snyder, S. *J. Nucl. Med.* **2010**, *51* (Suppl. 2), 480.
(23) Goda, K.; Bacso, Z.; Szabo, G. *Curr. Cancer Drug Targets* **2009**, *9*, 281.
(24) Inge, T. H.; Harris, N. L.; Wu, J. Q.; Azizkhan, R. G.; Priebe, W. *J. Surg. Res.* **2004**, *121*, 187.
(25) Kuss, B. J.; Corbo, M.; Lau, W. M.; Fennell, D. A.; Dean, N. M.; Cotter, F. E. *Int. J. Cancer* **2002**, *98*, 128.
(26) Goto, H.; Yang, B.; Petersen, D.; Pepper, K. A.; Alfaro, P. A.; Kohn, D. B.; Reynolds, C. P. *Mol. Cancer Ther.* **2003**, *2*, 911.
(27) Keshelava, N.; Groshen, S.; Reynolds, C. P. *Cancer Chemother. Pharmacol.* **2000**, *45*, 1.
(28) Tweddle, D. A.; Pearson, A. D. J.; Haber, M.; Norris, M. D.; Xue, C.; Flemming, C.; Lunec, J. *Cancer Lett.* **2003**, *197*, 93.